Nuclear Inst. and Methods in Physics Research, A 1029 (2022) 166453

Contents lists available at ScienceDirect

Nuclear Inst. and Methods in Physics Research, A

journal homepage: www.elsevier.com/locate/nima

The study of fluorescence response to energy deposition in the BGO calorimeter of DAMPE

Cong Zhao, Haoting Dai, Chengming Liu, Yifeng Wei, Yunlong Zhang *, Zhiyong Zhang, Libo Wu[1], Ying Wang, Xiaolian Wang, Zizong Xu, Guangshun Huang **

State Key Laboratory of Particle Detection and Electronics, University of Science and Technology of China, Hefei 230026, China
Department of Modern Physics, University of Science and Technology of China, Hefei 230026, China

ARTICLE INFO

Keywords:
DAMPE
BGO crystal
Laser test
Fluorescence quenching effect

ABSTRACT

The DArk Matter Particle Explorer (DAMPE) space mission is designed to measure cosmic rays and gamma rays. The key sub-detector of DAMPE is the Bismuth Germanium Oxide (BGO) Electromagnetic CALorimeter (ECAL), which measures the energies of electrons/gamma-rays ranging from 5 GeV–10 TeV. A laser test carried out to study the response of the BGO ECAL to up to ~TeV energy deposition revealed that the BGO fluorescence response retains linearity at laser energy deposition densities higher than that induced by a ~10 TeV electromagnetic shower. The energy measurements obtained from on-orbit data were also compared with Monte Carlo simulation results. The present study confirms that there is no fluorescence quenching effect in the DAMPE BGO ECAL.

1. Introduction

High-energy Cosmic-Ray Electrons and positrons (CREs) can be used as probes to study Galactic high-energy processes based on their characteristics of quickly losing energy during propagation and can reveal information on phenomena such as dark-matter particle annihilation or decay. The spectra of CREs in interstellar space have been measured directly in experiments such as PAMELA [1], AMS-02 [2], FERMI-LAT [3], and CALET [4] which have obtained accurate results in direct observation of CREs below TeV magnitude. However, there are relatively few results beyond this magnitude. Moreover, there is a potential risk for measurement above the TeV magnitude in that there is no available beam source for the accurate calibration of the calorimeter. In particular, the AMS-02 collaboration found that its calorimeter had a quenching effect on the fluorescence response of electrons above 250 GeV [5]. And it was the first observation of the fluorescence quenching effect in organic scintillating fiber caused by an ElectroMagnetic (EM) shower. The fluorescence quenching would happen when the ground states of luminescent center are locally exhausted. It causes that the fluorescence yield is no longer proportional to the deposited energies. This has aroused our interest as to whether there is quenching effect under high-energy EM showers in the calorimeter used in a similar experiment, the DArk Matter Particle Explorer (DAMPE).

DAMPE [6] is one of the four space science satellites within the Strategic Priority Science and Technology Projects of China, and was launched into a sun-synchronous orbit at an altitude of 500 km at the end of 2015. One of the main scientific objectives of DAMPE is to search for dark matter particles by measuring high-energy electrons/positrons up to 10 TeV [7]. The satellite carries a Plastic Scintillator Detector (PSD) [8–10], a Silicon–Tungsten tracKer–converter (STK) [11,12], a Bismuth Germanium Oxide (BGO) imaging calorimeter [13], and a NeUtron Detector (NUD) [14].

The BGO Electromagnetic Calorimeter (BGO ECAL), a key sub-detector of the DAMPE spectrometer, contains approximately 32 radiation lengths designed to measure the energy range from 5 GeV to 10 TeV of CREs precisely. The sensitive unit of the ECAL is inorganic material BGO, whose fluorescence quenching effect has been observed for low-energy hadrons and relativistic heavy ions with the high Linear Energy Transfer (LET) [15–17]. However, it is still unclear whether there is a quenching effect for ~ TeV EM showers with extremely high energy deposition densities.

This paper presents the results of a study in which a high-intensity laser was used to excite a BGO crystal to mimic the high densities of energy deposited by EM showers to check the linearity of the BGO fluorescence response to the energy deposited at the shower centers of 10 TeV-order electrons. The response of the BGO crystal to high-energy EM showers was also assessed through a comparison of data obtained from orbital CREs and Monte Carlo (MC) simulation.

* Corresponding author at: State Key Laboratory of Particle Detection and Electronics, University of Science and Technology of China, Hefei 230026, China.
** Corresponding author at: State Key Laboratory of Particle Detection and Electronics, University of Science and Technology of China, Hefei 230026, China.
E-mail addresses: ylzhang@ustc.edu.cn (Y. Zhang), hgs@ustc.edu.cn (G. Huang).
[1] Libo Wu is now at Gran Sasso Science Institute (GSSI), Via Iacobucci 2, I-67100 L'Aquila, Italy.

https://doi.org/10.1016/j.nima.2022.166453
Received 18 September 2021; Received in revised form 21 December 2021; Accepted 24 January 2022
Available online 16 February 2022
0168-9002/

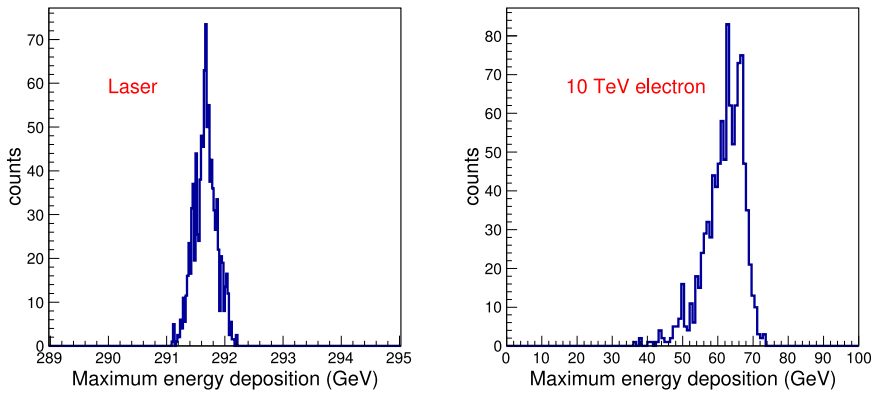

(a) (b)

Fig. 1. Maximum energy deposition distributions of (a) laser and (b) a set of 10 TeV electrons over a volume of 27 mm^3.

2. The BGO calorimeter

The BGO ECAL is a total absorption-type calorimeter composed of 308 BGO crystals. It contains seven coordinate planes (~32 radiation lengths, ~1.6 nuclear interaction lengths), each of which has two layers arranged orthogonally to provide measurement of shower profiles on the X–Y plane. Each layer consists of 22 BGO crystal bars with dimensions of 25 mm × 25 mm × 600 mm.

Each end of a BGO crystal is coupled to a PhotoMultiplier Tube (PMT) (Hamamatsu R5610A-01) [18]. The signals produced by the PMT are read out by three dynodes (dy2, dy5, and dy8 corresponding to low, medium, and high gain, respectively) to achieve a large dynamic range. The readout electronics uses VA160 and VATA160 Application Specific Integrated Circuits (ASICs) developed by IDE AS Inc. in Norway [19]. Each chip comprises 32 readouts with sensitivities of approximately 1 fC per ADC count and linear output to approximately 12 pC with an Integral NonLinearity (INL) of less than 2%. The output linearities of PMTs with their readout electronic chains were studied carefully in [20,21].

To further extend the dynamic range of the BGO crystal, the energy coverages of the two ends of a BGO crystal (named Side0 and Side1) are made to be slightly different by adjusting the filters between the PMT and BGO coupling end to make the amount of energy measurable by Side1 greater than that measurable by Side0 by a factor of five. The energy ranges [7] of different readout dynodes are listed in Table 1.

Based on the good linearity [20,21] of the output of the three dynodes of a PMT and its readout electronics, the fluorescence yield linearity of a BGO crystal was studied using a laser test platform comprising the BGO crystal, the PMT, and readout electronics equivalent to those used for the DAMPE detector. The output linearities of dy8, dy5, and dy2 were studied by using a laser to excite the BGO crystal. The output charge of dy2 at Side1 of the BGO crystal reached 12 pC (the upper limit of the VA160 chips linear response), corresponding to an energy deposition of about 4000 GeV, which is approximately equal to the energy deposited on a crystal located at the shower center produced by a 20 TeV electron as modeled by MC simulation. Therefore, our focus was on studying the output linearity of the three dynodes of Side1, particularly on whether the charge signal readout of dy2 could linearly reach 12 pC.

Table 1
Deposited energies obtained from different readout dynodes.

Side	Dynode		
	2	5	8
0	3.2 GeV–800 GeV	80 MeV–20 GeV	2 MeV–500 MeV
1	16 GeV–4000 GeV	400 MeV–100 GeV	10 MeV–2.5 GeV

3. Laser test

3.1. Simulation of energy deposition density

Although the mechanisms through which fluorescence is produced in BGO crystals by lasers and EM showers may be different, in both cases the excitation of ground state for luminescent center is generated by the consumption of deposited energy thereby inducing fluorescence. The energy deposition behavior of secondary electrons and photons from EM shower is quite similar to that of laser photons, which differs from that of high LET nuclides. A laser pulse produces the same amount of energy deposition but with a larger volume density of energy deposition in the test crystal than that in the crystal located at the shower center of a 10 TeV electron. The response of the test crystal to the laser reflects whether BGO ECAL has a linear fluorescence response to TeV-order EM shower. The detailed discussion of energy deposition density is shown below. A high-intensity laser, Opolette 355 LD OPO system (Opotek Inc.) [22] was used to excite the BGO crystal. The Opolette tunable laser generates wavelengths over a broad range from 210 to 2400 nm. The BGO crystal characteristics were measured under excitation by a 310 nm wavelength light pulse with a spot radius of less than 2 mm and a pulse width of less than 7 ns. The signal pulse energy was ~2 mJ and the pulse repetition rate was 1 Hz. To evaluate whether the energy density deposited in the BGO crystal by the laser matched that of a 10 TeV electron shower center, an MC simulation was carried out using the Geant4 toolkit [22]. For the laser simulation, a 310 nm laser beam (4 eV per photon) with a 2 mm spot radius, which is consistent with the practical conditions, was generated. Nearly 8×10^{11} photons were generated to hit the BGO crystal of these, approximately 5×10^{11} photons were absorbed by the tested crystal, resulting in a total deposited energy per pulse equal to 2 TeV, which is the same as the energy deposited on the bar located at the shower center of BGO ECAL by a 10 TeV electron. Considering that the energy deposition density of an electron increases closer to the shower center, we calculated the energy deposition densities over different volumes around the shower center and compared the results with those produced by the laser. As an example, Fig. 1(a) provides the energy deposition distribution of the laser over a BGO volume of 27 mm^3 at the first 2.15 mm depth and 2 mm radius and Fig. 1(b) provides the energy deposition distribution of a set of 10 TeV MC electrons over a BGO volume of 27 mm^3 within the shower central region. The energies deposited by the laser and a 10 TeV electron are 291.7 (energy deposition density of 10.8 GeV/mm^3) and 61.9 GeV (energy deposition density of 2.3 GeV/mm^3), respectively. The energy deposition densities over different volumes are listed in Table 2. The results suggest that the energy deposition density of the laser is larger

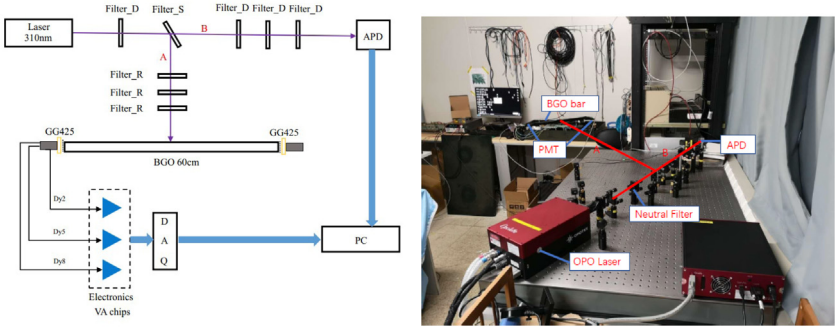

(a) (b)

Fig. 2. Experimental setup: (a) schematic diagram, and (b) practicality picture.

Table 2
Maximum energy deposition densities of electron and laser over different volumes.

Volume (mm^3)	Laser (GeV/mm^3)	Electron (GeV/mm^3)
125	8.9	1.2
27	10.8	2.3
1	11.4	7.9

than that of electron even at a scale of 1 mm^3, in which the energy deposition of a 10 TeV electron onto the BGO crystal is only 7.9 GeV, far less than the resolution of the BGO ECAL. The energy deposition density of the laser used in the experiment was therefore sufficient to imitate that of a 10 TeV electron.

3.2. Laser test setup

The laser experimental setup is shown in Fig. 2. The neutral filters on the optical path, Filter_S, Filter_D and Filter_R, were used to divide the laser and attenuate its intensity. Filter_S was primarily used to divide the laser into Channels A and B, with Channel A used to excite the BGO crystal. The PMTs and PMT readout electronics were the same as those used by DAMPE in orbit with the exception that a long pass filter (GG425 filter, Schott Corporation) was placed between the BGO crystal and the PMT to keep the 310 nm laser from directly entering the PMT. Channel B directly injected on to an Avalanche PhotoDiode (APD, Hamamatsu S8664-1010) [23] with readout electronics described in [24]. The APD was used to monitor the laser intensity during the test. Filter_D was adjusted to ensure that the laser intensity entering the APD was to produce a signal fall in its electronic linear region. To synchronize the data acquisition, a trigger signal was sent to the APD acquisition system from the Data AcQuisition (DAQ) board of the BGO. The laser intensity could be tuned easily by the control software.

3.3. Results

From the results of a ground cosmic muon study [20], the corresponding relationships between the output charge (ADC channels) of each dynode and the deposited energy were obtained. Laser intensity was found to gradually increase until the output charges of dy8, dy5, dy2 of PMT at Side1 reaches at least 12 pC. The correlations between the PMT and APD signals are plotted in Fig. 3 on which the x-axis represents the output of the APD, and the *y*-axis represents the signal measured by the dynodes. Fig. 3(a), 3(b), and 3(c) present the outcomes for dy8, dy5, and dy2 of PMT at Side1, respectively. As detailed in Fig. 3(c), the dy2 varies from several hundred up to ~12000 ADC channels under the different energy deposits. The result shows that dy2 provides a linear response of charge output over a dynamic range from several tens of fC to 12 pC, which corresponds to BGO energy deposits from several tens of GeV to ~4 TeV. The response linearities of energy

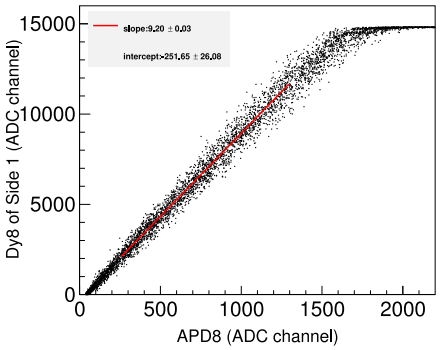

(a)

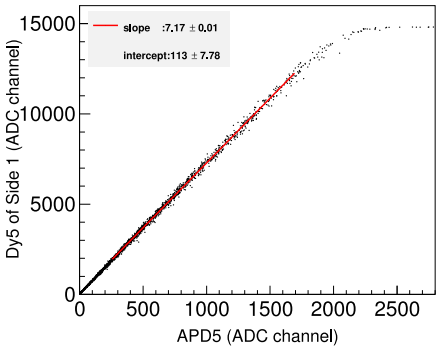

(b)

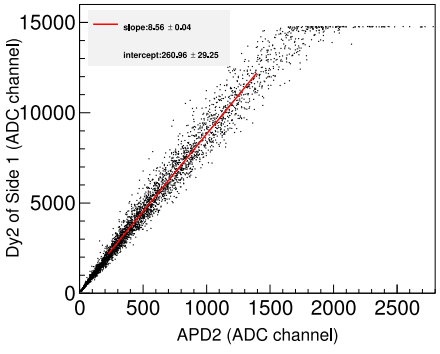

(c)

Fig. 3. Relation between output of each dynode of PMT at Side1 and APD. Red lines are linear fitted functions. (a) Dy8 of PMT at Side1 versus APD8. (b) Dy5 of PMT at Side1 versus APD5. (c) Dy2 of PMT at Side1 versus APD2.

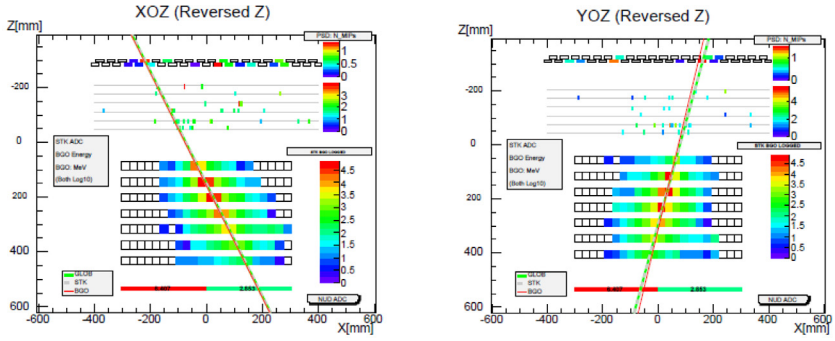

(a) (b)

Fig. 4. Example of a high-energy CREs candidate event in (a) XOZ and (b) YOZ planes of DAMPE. The BGO crystal bars of neighboring layers are alternated orthogonally to image the shower profile. The XOZ and YOZ planes are defined as side views vertical to the odd and even layers (numbered from 0), respectively.

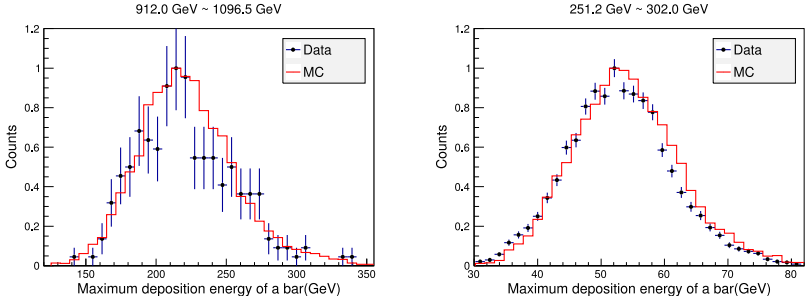

(a) (b)

Fig. 5. Deposited energy distributions in BGO bars located at EM shower centers induced by electrons with energies of (a) 251.2–302 GeV; (b) 1096.5–1318.3 GeV. Black dots with error bars indicate flight data; red lines indicate MC simulation.

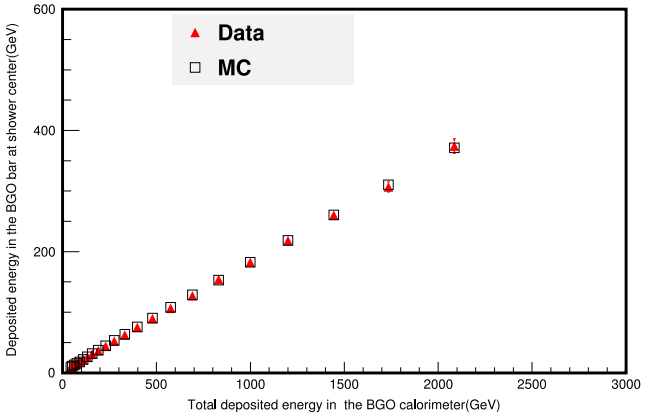

Fig. 6. Energy deposited in BGO bar located at EM shower center plotted against total deposited energy. Flight data are indicated by red triangles; MC simulations are indicated by open black squares.

deposition at lower energies are shown in Figs. 3(b) and 3(a). It is seen that the fluorescence response in the energy measurement range of the BGO is linear with the laser excitation at energy deposition densities higher than that in the shower center of a 10 TeV electron. These laser test results indicate that there is no fluorescence quenching effect in a BGO crystal located at the shower center of a 10 TeV-order electron.

4. Energy response of the BGO crystal to electrons

To further validate the laser test results, energy measurements obtained from CREs using DAMPE in orbit were studied. The shower profile of a high-energy CREs candidate event observed in orbit with DAMPE is shown in Fig. 4. The energy deposition in the BGO crystal located at the shower center was analyzed and compared with the results of MC simulation without a fluorescence quenching effect using GEANT4.10.02 with the physics list FTFP-BERT. The simulated electron spectrum is sampled according to the outcomes of in-orbit observation [25]. Fig. 5 shows the energy deposition distributions of CREs on a BGO bar located at the shower center, with the black dots representing orbital data and the solid line showing simulation results. The simulation and flight data are both fitted by Gaussian functions. For electron candidates with total deposited energies in the 251.2–302.0 GeV interval (Fig. 5(a)), the mean values of the simulation and flight data are 53.3 ± 0.1 and 52.5 ± 0.1 GeV, respectively. For electron candidates with total deposited energies in the 1096.5–1318.3 GeV interval (Fig. 5(b)), the mean values of the simulation and flight data are 219.7 ± 0.4 and 218.2 ± 2.8 GeV, respectively. Fig. 6 shows the correlation between the total deposited energy in DAMPE and the deposited energy in the BGO bar located at the EM shower center, in which the red triangles indicate orbit data and the open black squares indicate MC simulation results. The results demonstrate that the energy reconstruction of the BGO ECAL is valid within the TeV energy region. The consistency between the orbital and MC results, further verifies that there is no fluorescence quenching effect in a BGO crystal located at an EM shower center produced by an electron with a total deposited energy up to the TeV range.

5. Conclusion

The response of a BGO crystal located at the EM shower center of a high-energy CRE in orbit was studied using a high-intensity laser system in the laboratory. The experimental results indicate that there is

no quenching effect when the energy peak density of the laser exceeds that induced by a 10 TeV EM shower. Further study on the deposited energy distributions of BGO bars located at EM shower centers induced by electron candidates with total deposited energies of up to several TeV revealed that the flight data are consistent with MC simulation results with no fluorescence quenching effect.

CRediT authorship contribution statement

Cong Zhao: Formal analysis, Data curation, Investigation, Writing – original draft. **Haoting Dai:** Methodology, Validation. **Chengming Liu:** Formal analysis, Validation. **Yifeng Wei:** Validation, Funding acquisition. **Yunlong Zhang:** Writing – review & editing, Conceptualization, Supervision, Funding acquisition. **Zhiyong Zhang:** Validation, Funding acquisition. **Libo Wu:** Validation. **Ying Wang:** Validation. **Xiaolian Wang:** Conceptualization. **Zizong Xu:** Conceptualization. **Guangshun Huang:** Supervision, Funding acquisition.

Declaration of competing interest

The authors declare that they have no known competing financial interests or personal relationships that could have appeared to influence the work reported in this paper.

Acknowledgments

This work is supported by the Joint Funds of the National Natural Science Foundation of China (Grant No. U1738208, U1738139, U1738135, and 11851302), the Outstanding Youth Science Foundation of NSFC (Grant No. 12022503), the National Natural Science Foundation of China (Grant No. 11673021 and 11705197), the National Key Research and Development Program of China (Grant No. 2016YFA0400200), and the Youth Innovation Promotion Association CAS, China (Grant No. 2921450).

References

[1] P. Picozza, A. Galper, G. Castellini, O. Adriani, F. Altamura, M. Ambriola, G. Barbarino, A. Basili, G. Bazilevskaja, R. Bencardino, et al., PAMELA–A Payload for antimatter matter exploration and light-nuclei astrophysics, Astropart. Phys. 27 (4) (2007) 296–315.

[2] R. Battiston, The antimatter spectrometer (AMS-02): A particle physics detector in space, Nucl. Instrum. Methods Phys. Res. A 588 (1) (2008) 227–234.

[3] W. Atwood, A.A. Abdo, M. Ackermann, W. Althouse, B. Anderson, M. Axelsson, L. Baldini, J. Ballet, D. Band, G. Barbiellini, et al., The large area telescope on the Fermi gamma-ray space telescope mission, Astrophys. J. 697 (2) (2009) 1071.

[4] S. Torii, C. Collaboration, et al., The CALET experiment on ISS, Nuclear Phys. B Proc. Suppl. 166 (2007) 43–49.

[5] A. Kounine, Z. Weng, W. Xu, C. Zhang, Precision measurement of 0.5 GeV–3 TeV electrons and positrons using the AMS electromagnetic calorimeter, Nucl. Instrum. Methods Phys. Res. A 869 (2017) 110–117.

[6] J. Chang, Dark matter particle explorer: The first chinese cosmic ray and hard γ-ray detector in space, Chin. J. Space Sci. 34 (5) (2014) 550–557.

[7] J. Chang, G. Ambrosi, Q. An, R. Asfandiyarov, P. Azzarello, P. Bernardini, B. Bertucci, M. Cai, M. Caragiulo, D. Chen, et al., The dark matter particle explorer mission, Astropart. Phys. 95 (2017) 6–24.

[8] Y. Yu, Z. Sun, H. Su, Y. Yang, J. Liu, J. Kong, G. Xiao, X. Ma, Y. Zhou, H. Zhao, et al., The plastic scintillator detector for DAMPE, Astropart. Phys. 94 (2017) 1–10.

[9] Y. Zhou, Z. Sun, Y. Yu, Y. Zhang, F. Fang, J. Chen, B. Hu, A large dynamic range readout design for the plastic scintillator detector of DAMPE, Nucl. Instrum. Methods Phys. Res. A 827 (2016) 79–84.

[10] M. Ding, Y.-P. Zhang, Y.-J. Zhang, Y.-P. Wang, T.-K. Dong, A. De Benedittis, P. Bernardini, F. Fang, Y. Li, J. Liu, et al., Calibration of the DAMPE plastic scintillator detector and its on-orbit performance, Res. Astron. Astrophys. 19 (3) (2019) 047.

[11] P. Azzarello, G. Ambrosi, R. Asfandiyarov, P. Bernardini, B. Bertucci, A. Bolognini, F. Cadoux, M. Caprai, I. De Mitri, M. Domenjoz, et al., The DAMPE silicon–tungsten tracker, Nucl. Instrum. Methods Phys. Res. A 831 (2016) 378–384.

[12] F. Zhang, W.-X. Peng, K. Gong, D. Wu, Y.-F. Dong, R. Qiao, R.-R. Fan, J.-Z. Wang, H.-Y. Wang, X. Wu, et al., Design of the readout electronics for the DAMPE silicon tracker detector, Chin. Phys. C 40 (11) (2016) 116101.

[13] Z. Zhang, C. Wang, J. Dong, Y. Wei, S. Wen, Y. Zhang, Z. Li, C. Feng, S. Gao, Z. Shen, et al., The calibration and electron energy reconstruction of the BGO ECAL of the DAMPE detector, Nucl. Instrum. Methods Phys. Res. A 836 (2016) 98–104.

[14] Y.-Y. Huang, T. Ma, C. Yue, Y. Zhang, M.-S. Cai, J. Chang, T.-K. Dong, Y.-Q. Zhang, Calibration and performance of the neutron detector onboard of the DAMPE mission, Res. Astron. Astrophys. 20 (9) (2020) 153.

[15] E. Valtonen, J. Peltonen, J.J. Torsti, Response of BGO and CsI (Tl) scintillators to heavy ions, Nucl. Instrum. Methods Phys. Res. A 286 (1–2) (1990) 169–174.

[16] E. Bakkum, C. Van Engelen, R. Kamermans, T. Teeling, L. Timmerman, The response of BGO scintillation detectors to light charged particles, Nucl. Instrum. Methods Phys. Res. 225 (2) (1984) 330–334.

[17] Y. Wei, Y. Zhang, Z. Zhang, L. Wu, H. Dai, C. Liu, C. Zhao, Y. Wang, Y. Zhao, P. Jiang, et al., The quenching effect of BGO crystals on relativistic heavy ions in the DAMPE experiment, IEEE Trans. Nucl. Sci. 67 (6) (2020) 939–945.

[18] https://www.hamamatsu.com/resources/pdf/etd/PMT_TPMZ0002E.pdf.

[19] https://ideas.no.

[20] Z. Zhang, Y. Zhang, J. Dong, S. Wen, C. Feng, C. Wang, Y. Wei, X. Wang, Z. Xu, S. Liu, Design of a high dynamic range photomultiplier base board for the BGO ECAL of DAMPE, Nucl. Instrum. Methods Phys. Res. A 780 (2015) 21–26.

[21] C. Feng, D. Zhang, J. Zhang, S. Gao, D. Yang, Y. Zhang, Z. Zhang, S. Liu, Q. An, Design of the readout electronics for the BGO calorimeter of DAMPE mission, IEEE Trans. Nucl. Sci. 62 (6) (2015) 3117–3125.

[22] S. Agostinelli, J. Allison, K.a. Amako, J. Apostolakis, H. Araujo, P. Arce, M. Asai, D. Axen, S. Banerjee, G. Barrand, et al., GEANT4—a simulation toolkit, Nucl. Instrum. Methods Phys. Res. A 506 (3) (2003) 250–303.

[23] https://www.hamamatsu.com/resources/pdf/ssd/e03_handbook_si_apd_mppc.pdf.

[24] L. Luo, Z. Shen, Y. Huang, Z. Jia, C. Feng, S. Liu, Design and optimization of the CSA-based readout electronics for STCF ECAL, J. Instrum. 15 (09) (2020) C09002.

[25] G. Ambrosi, Q. An, R. Asfandiyarov, P. Azzarello, P. Bernardini, B. Bertucci, M. Cai, J. Chang, D. Chen, H. Chen, et al., Direct detection of a break in the teraelectronvolt cosmic-ray spectrum of electrons and positrons, Nature 552 (7683) (2017) 63.